communications biology

Article

https://doi.org/10.1038/s42003-024-06622-7

Outer membrane vesicles from commensal microbes contribute to the sponge *Tedania* sp. development by regulating the expression level of apoptosis-inducing factor (AIF)

Check for updates

Kai Wang [1] ✉, Chenzheng Jia[1] ✉, Beibei Zhang[1] ✉, Jun Chen[1] ✉ & Jing Zhao [1,2,3] ✉

The transition from the swimming larval stage to the settlement stage represents a significant node in the marine sponge developmental process. Previous research has shown that the outer membrane vesicles (OMVs) from the bacterial species *Tenacibaculum mesophilum* associated with the sponge *Tedania* sp. influence larval settlement: low concentrations of OMVs increase the attachment rate, whereas high concentrations decrease the attachment rate. Here, by comparing the transcriptomes of sponge larvae in filtered seawater (FSW group) and in FSW supplemented with OMVs (FSW-OMV group), the results indicated that bacterial OMVs affected larval settlement by modulating the expression levels of apoptosis-inducing factor (AIF) in the host. Subsequently, quantitative real-time PCR revealed a decrease in *aif* expression near the time of settlement (SE) compared to that in the control group. RNA interference (RNAi) was used to target the *aif* gene, and the rate of larval settlement was significantly reduced, confirming the inhibitory effect of high concentrations of OMVs. Moreover, small RNA (sRNA) sequencing of OMVs revealed the existence of abundant AIF-sRNAs of 30 nt, further suggesting that one pathway for the involvement of sponge-associated bacteria in host development is the transport of OMVs and the direct function of cargo loading.

Marine benthic ecosystems play an integral role in important ecosystem functions from intertidal to deepest depths[1]. However, the development and maintenance of benthic marine animal assemblages are highly reliant on the successful recruitment of swimming larvae[2]. Many marine organisms release larvae into the water column, where they spread to support remote populations and colonize new sites[3]. Locating suitable locations for larval settlement may be a crucial problem for larval survival, growth, and reproduction. Marine sponges are among the oldest metazoan animals and are sessile filter-feeder benthic invertebrates that predominate on a variety of hard-bottom substrates[4,5]. Most of the approximately 15,000 sponge species are marine, while a few can be found in brackish water, and approximately 150 species live in freshwater[6]. Similar to other marine invertebrates, sponges have an ancient and conserved biphasic life cycle, from a free-swimming phase to settlement and metamorphosis. Larval settlement is an important node in the growth and development process of the sponge, during which sponge larvae experience major developmental, morphological, physiological, and ecological changes[7].

Microbial species or communities are involved in the larval settlement of sponges and consequently, in their ecology and evolution, a process that pioneers studied decades ago[8,9]. Increasing evidence has emphasized the possibility that sponge-associated microorganisms develop different strategies to aid larval settlement, such as forming biofilms and producing bioactive materials[10]. Biofilms are believed to facilitate larval settlement

[1]College of Ocean and Earth Science of Xiamen University, Xiamen, 361005, China. [2]Xiamen City Key Laboratory of Urban Sea Ecological Conservation and Restoration (USER), Xiamen University, Xiamen, 361005, China. [3]State Key Laboratory of Mariculture Breeding, College of Ocean and Earth Sciences, Xiamen University, Xiamen, 361102, China. ✉e-mail: 22320200155959@stu.xmu.edu.cn; czjia@stu.xmu.edu.cn; 22320210156210@stu.xmu.edu.cn; chenjun@xmu.edu.cn; sunnyzhaoj@xmu.edu.cn

because they are composed of various components, including bacteria and diatoms, extracellular polymeric substances, quorum sensing signals, unique inductive compounds, and exoenzymes[11]. Recent research has shown that the precursor arginine in the nitric oxide (NO) pathway, a signaling molecule linked to larval settlement, is produced by sponge symbiotic microorganisms[12,13]. Whether through biofilms or signaling molecules, the acquisition of certain extracellular components derived from microorganisms may be important in helping larvae to settle successfully[14,15].

OMVs are lipid bilayer-coated nanoscale membrane vesicles that enable active intercellular communication by breaking the boundary between cells[16]. OMVs can transport a wide variety of cargos from microorganisms to the host and participate in host development[17,18]. In complex marine environments, which include abundant organisms and various organic matter, OMVs from marine bacteria could protect and condense biomaterials to create a relatively stable transport channel for host-microbe cell interactions. OMVs from *Pseudoalteromonas marina* were found to significantly enhance plantigrade settlement in the mussel *Mytilus coruscus* via the transport of lipopolysaccharides (LPS)[19]. *Vibrio fischeri*-derived OMVs also make significant contributions to the development of squid light organs via the transport of peptidoglycan (PG) and LPS[20]. Signaling lipids found in the OMVs of *Algoriphagus machipongonensis* induce rosette formation of the choanoflagellate *Salpingoeca rosetta*[21]. Despite being less explored, the transport of various signaling molecules by molecular cargo-carrying OMVs has been shown to be a typical biological trait[22]. Sponge-microbe interactions are not exclusively mutualistic; here, the bacterial OMVs could shield potential effector molecules from the negative effects of enzymes, allowing them to be targeted to host cells[23].

In addition, cargos have also been shown to have direct effects, e.g., sRNAs originating from tRNA fragments can regulate multiple mRNA targets, similar to microRNAs in eukaryotes[24,25]. OMVs from *Escherichia coli* carrying abundant very small RNAs can be transferred to human HCT116 cells and promote MAP3K4 expression[26]. When *V. fischeri* transits from its environmental reservoir to its host squid *Euprymna scolopes*, bacterial OMVs upregulate the transcription of the outer membrane protein OmpU in the host[27]. OMVs from *Proteus mirabilis* downregulated miR-96-5p, which caused an increase in Abca1 expression and mitochondria-dependent apoptosis, ultimately inhibiting osteoclastogenesis and bone loss[28]. Limited study has indicated that bacterial OMVs can directly participate in the transcriptional regulation of the host, thereby affecting the growth and development of the host. Here, considering that sponge larval settlement is a developmental process accompanied by cell differentiation and recombination, apoptosis could play an essential role in clearing redundant or abnormal cells in organisms via OMVs[29].

In a previous study, we found that OMVs from Bacteroidetes species ranged in size from 50–200 nm and contained effective components to facilitate the settlement of sponge larvae, significantly increasing the larval settling rate[30]. Nevertheless, the intricate mechanisms of the interaction between microbes and sponge larvae are rather unclear. In this study, we further investigated which cargo was transported via OMVs and which pivotal signaling pathway was affected during larval settlement. Through a comparative transcriptome analysis of different phases of sponge larval development, we focused on the apoptosis signaling pathway. Moreover, the sRNAome analysis of bacterial OMVs revealed the presence of AIF-sRNAs, which are key genes in the apoptosis signaling pathway. Quantitative real-time PCR (qRT–PCR) and RNA interference (RNAi) experiments indicated that sRNAs carried by OMVs could change the transcriptional landscape of host cells, consequently affecting the apoptosis signaling pathway to induce larval settlement. These results reveal the potential and importance of microorganisms regulating the growth and development of marine invertebrates and offer a new way to study symbiotic interactions based on bacterial OMV-sRNAs.

Results

Comparative transcriptomic analysis of *Tedania* sp. larvae treated with bacterial OMVs

In this study, the attachment rate of larvae increased with time and varied under different concentrations of OMVs at each time point. At the 9th hour, nearly 70% of the sponge larvae with OMVs addition had successfully settled on the substrate, and the percentage in the FSW group reached the highest level but less than 40%. Lower OMVs abundance with 0.08 μg/ml and 0.8 μg/ml protein concentration, promoted larval settlement, while a higher OMVs concentration (8 μg/ml), conversely inhibited larval settlement (Fig. 1a). Sponge larvae were divided into two groups (FSW and FSW-OMV groups) (Fig. 1b) and a comparative transcriptomic analysis was performed to better understand how bacterial OMVs influence the larval settling process at the molecular level. A total of 613 million reads for all samples were obtained by transcriptome sequencing, and the completeness of the assembled transcriptome was assessed against the metazoan reference data (BUSCO) (Supplementary Fig. S1). After removing the reads of adapters, reads of poly A sequences and low-quality reads with a quality score < 20, more than 608 million high-quality reads remained for further analysis. The average number of raw data, filtered data, GC content, number of mapped reads and mapping rate for the samples are shown in Supplementary Table S1, and these data indicated no sequence contamination during the sequencing process. From each stage, a total of 65.02–76.19% of the reads were mapped to the *Tedania* sp. full-length transcriptome, and the average coverage of the transcripts was approximately 74% in the gene model (Supplementary Fig. S2 and Table S2). A number of genes displayed saturation tendencies, and all samples were distributed in a homogeneous and random manner, meeting the requirements of the next analysis (Supplementary Fig. S3 and Table S3). Principal component analysis (PCA) of the transcriptomic reads revealed that the first two PCs explained most of the variance (80.4% and 8.9%, respectively) (Fig. 1c). Fifteen samples were grouped into three distinct clusters that were correlated with the three developmental stages and had reliable repeatability. The samples from the same phase clustered together, such as CR-OMV (critical larva with OMVs addition) and CR-FSW (critical larva without OMVs), as well as SE-OMV (settled larva with OMVs) and SE-FSW (settled larva without OMVs). A cluster heatmap plot further showed a strong correlation between samples from the same developmental stage (Fig. 1d). It also indicated that the differences in overall gene expression among the three developmental stages were more significant than those from samples with or without OMVs addition. These results suggested that the addition of OMVs did not change the growth situation of larvae at sampling time (6th and 9th hour) but could influence the larval attachment rate.

Analysis of DEGs among the larval developmental stages following bacterial OMVs addition

An analysis of differentially expressed genes was conducted during the three developmental stages of *Tedania* sp. larvae using the software package DESeq2. In total, 30,979 distinct genes were identified as expressed (Supplementary Table S4), and the significantly differentially expressed genes (DEGs) that met the filtering criteria (FDR < 0.05 and fold changes >2) were selected. The number of DEGs varied among the different groups, ranging from 29 DEGs (SE-FSW-vs.-SE-OMV) to 17119 DEGs (SW-vs.-CR-FSW) (Fig. 2a). This comprehensive analysis revealed that the number of DEGs varied significantly during growth and development rather than during OMVs addition, although the addition of OMVs resulted in a small number of DEGs (CR-FSW-vs.-CR-OMV and SE-FSW-vs.-SE-OMV). Then, Venn diagrams of the DEGs in the five experimental groups showed that SW, CR-FSW, CR-OMV, SE-FSW and SE-OMV shared 13,473 common DEGs from the swimming to settlement stages (Fig. 2b). Two hundred specific DEGs were expressed at the SW stage, 176 at the CR-OMV stage, 459 at the CR-FSW stage, 245 at the SE-FSW stage and 773 at the SE-OMV stage. Notably, the greatest number of DEGs in the SE-OMV group showed that OMVs addition contributed to more genes or pathways in the SE phase

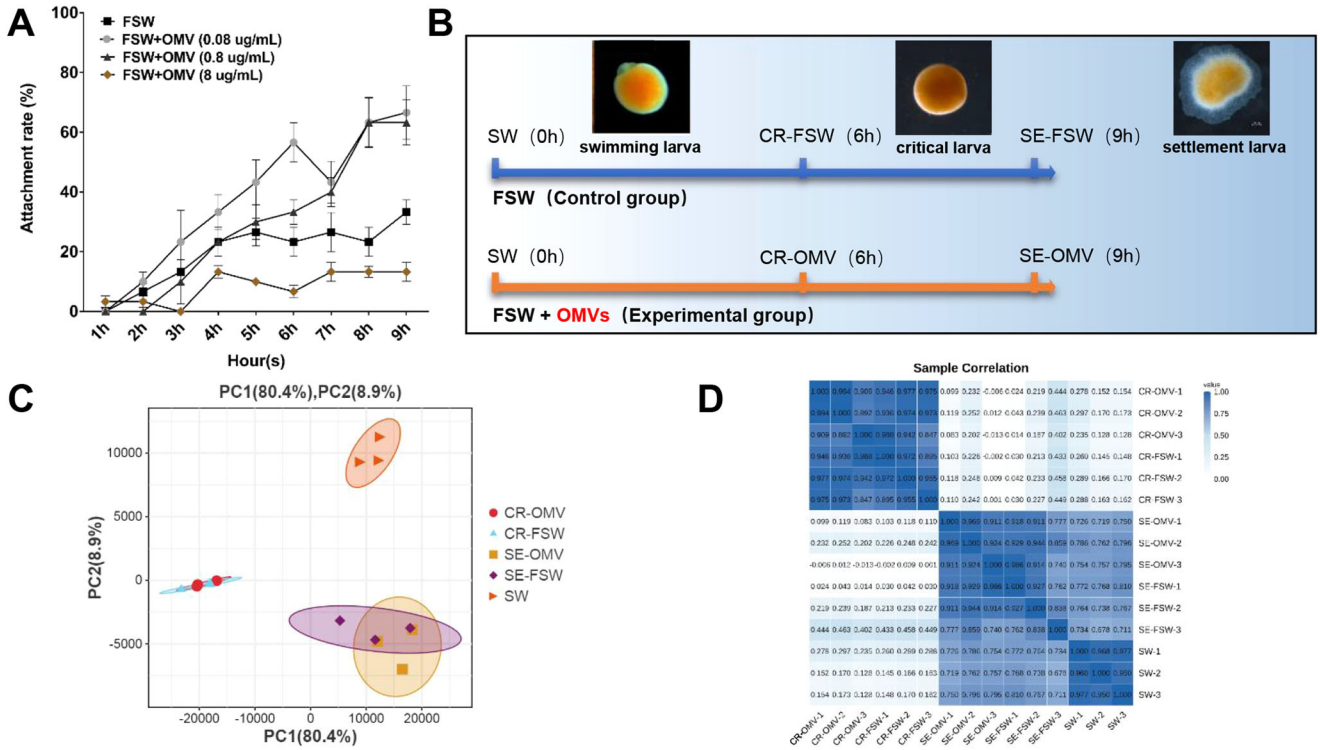

Fig. 1 | Transcriptomic analysis of OMVs inducing the settlement of *Tedania* sp. larvae. A Larval settlement assay of *Tedania* sp. with or without OMVs addition. Error bars represent one standard deviation from the mean of biological triplicate samples. **B** Samples were collected for the transcriptome analysis. SW: swimming larva; CR: critical larva; SE: settlement larva. **C** Principal component analysis of different stages of larval development. **D** Sample relationship heatmap plotting different stages of larval development. Dark blue represents a strong correlation, light blue represents a weak correlation, and each column and row corresponds to the relationships of one sample with the other 15 samples, including itself.

(SE-FSW-vs.-SE-OMV). According to GO enrichment analyses, the majority of DEGs affected by OMVs in the CR developmental stage (CR-FSW-vs.-CR-OMV) were associated with ion transmembrane transport (GO:0034220), hydrogen peroxide biosynthetic process (GO:0050665), cytoplasm (GO:0005737) and intrinsic component of membrane (GO:0031224) (Fig. 2c). The DEGs from OMVs group in the SE developmental stage (SE-FSW-vs.-SE-OMV) were clustered in the ion transmembrane transport (GO:0034220), regulation of embryonic development (GO:0045995), cell development (GO:0048468), regulation of cysteine-type endopeptidase activity (GO:2000116) and intrinsic component of membrane (GO:0031224) terms. These results indicated that DEGs induced by OMVs addition during the CR stage were mainly related to ion transmembrane transport and energy metabolism, while DGEs detected during the SE stage were involved in cell development. A further cluster analysis of the enriched KEGG pathways revealed that the addition of bacterial OMVs affected oxidative phosphorylation (ko00190) and metabolic pathways (ko01100) (Fig. 2d). Notably, at the SE developmental stage, the apoptosis-fly pathway (ko04214) in the OMVs group was of interest. The KEGG enrichment analysis of the top 20 DEGs revealed that the primary effect of OMVs was on the regulation of oxidative phosphorylation and the apoptosis signaling pathway (Fig. 2e, Supplementary Fig. S4). By integrating GO and KEGG analyses, we speculated that bacterial OMVs could play roles in energy metabolism during the CR stage by modulating oxidative phosphorylation, and in cell development during the SE stage by regulating the apoptosis signaling pathway.

AIF (apoptosis-inducing factor) is related to bacterial OMVs regulating apoptosis

Subsequently, a total of 29 DEGs (SE-FSW-vs.-SE-OMV, Fig. 2a) were linked to the regulation of larval attachment via bacterial OMVs, but most of these DEGs could not be identified due to the lack of genomic references in sponges. Finally, 3 annotated DEGs were identified at the SE developmental node (SE-FSW-vs.-SE-OMV), which were enriched in oxidative phosphorylation, metabolic pathways and apoptosis-fly. Importantly, *aifm1* (AIF) was identified as the sole pivotal DEG in the apoptosis signaling pathway. The amino acid sequence of *Te*-AIF showed 50.49% similarity to those of other AIFs in marine animals (Supplementary Fig. S5). However, *Te*-AIF was located on one separate branch of the marine sponge, close to the sponges *Suberites domuncula* and *Amphimedon queenslandica*, which are distinct from AIF sequences from other species in an evolutionary tree (Fig. 3a). The expression patterns of DEGs related to the five experimental groups further indicated that *aifm1* was downregulated at the SE-OMV stage (Fig. 3b). Furthermore, the qRT-PCR results confirmed that the expression of the *aif* gene continued to increase from the SW to CR to SE stages, particularly in the latter developmental process from CR to SE, with a significant increase in the expression of the *Te-aif* gene in the FSW sample (SE-FSW). However, in contrast to that in the control group, *aif* expression was downregulated at the SE stage (SE-OMV) with OMVs addition (Fig. 3c). An RNAi assay was subsequently performed to validate the role of *Te-aif* in the larval settlement process. Nine hours after AIF-siRNA was added, *Te-aif* was successfully knocked down compared with that in the FSW and dsGFP control groups (Fig. 3d). Interestingly, larval settlement was influenced when *Te-aif* was knocked down, and the larval attachment rate (dsAIF: 11.25%) decreased significantly compared with that of the other two groups (FSW: 54.82%, dsGFP: 41.78%), confirming the inhibitory effect of high concentrations of OMVs. A comparison of the concentration of OMVs in the OMV-mediated group (Fig. 1a) and the *aif* expression level in larvae from the RNAi knockdown group (Fig. 3d) suggested that the expression of the *aif* gene needs to be regulated within an optimal range that could promote larval settling, while excessive or insufficient expression of *aif* could hinder the settlement process.

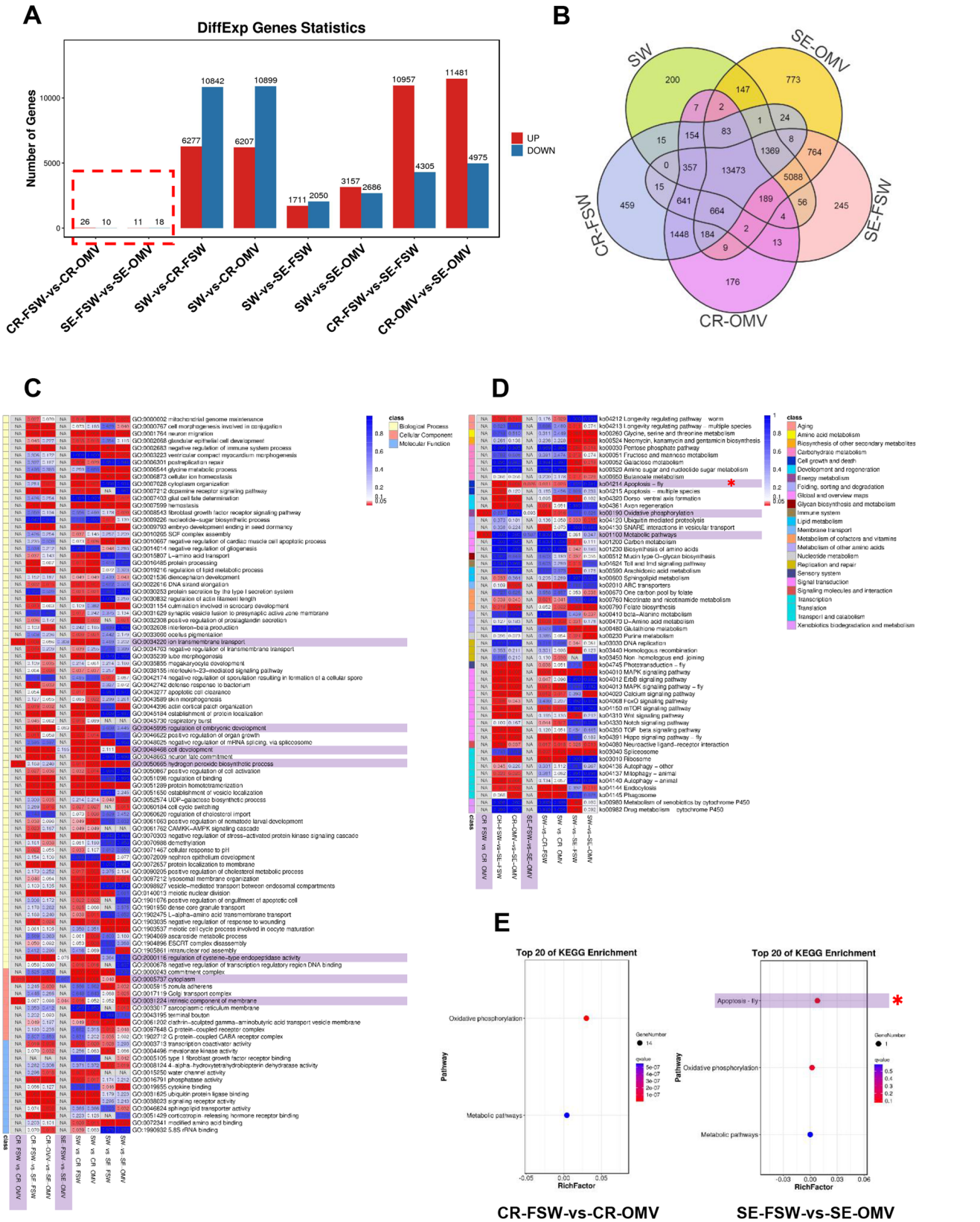

Fig. 2 | Identification and enrichment analysis of DEGs in sponge larvae from the swimming to settlement stages after OMVs addition. A The number of DEGs obtained from comparisons of CR-FSW-vs.-CR-OMV, SE-FSW-vs.-SE-OMV, SW-vs.-CR-FSW, SW-vs.-CR-OMV, SW-vs.-SE-FSW, SW-vs.-SE-OMV, CR-FSW-vs.-SE-FSW and CR-OMV-vs.-SE-OMV. **B** Venn diagrams of the DEGs identified in the five developmental stages. **C** GO enrichment analysis of the DEGs. **D** KEGG enrichment analysis of the DEGs. The color indicates the strength of significance, with the color approaching red representing stronger significance. **E** Top 20 enriched KEGG pathways in the comparisons of CR-FSW-vs.-CR-OMV and SE-FSW-vs.-SE-OMV.

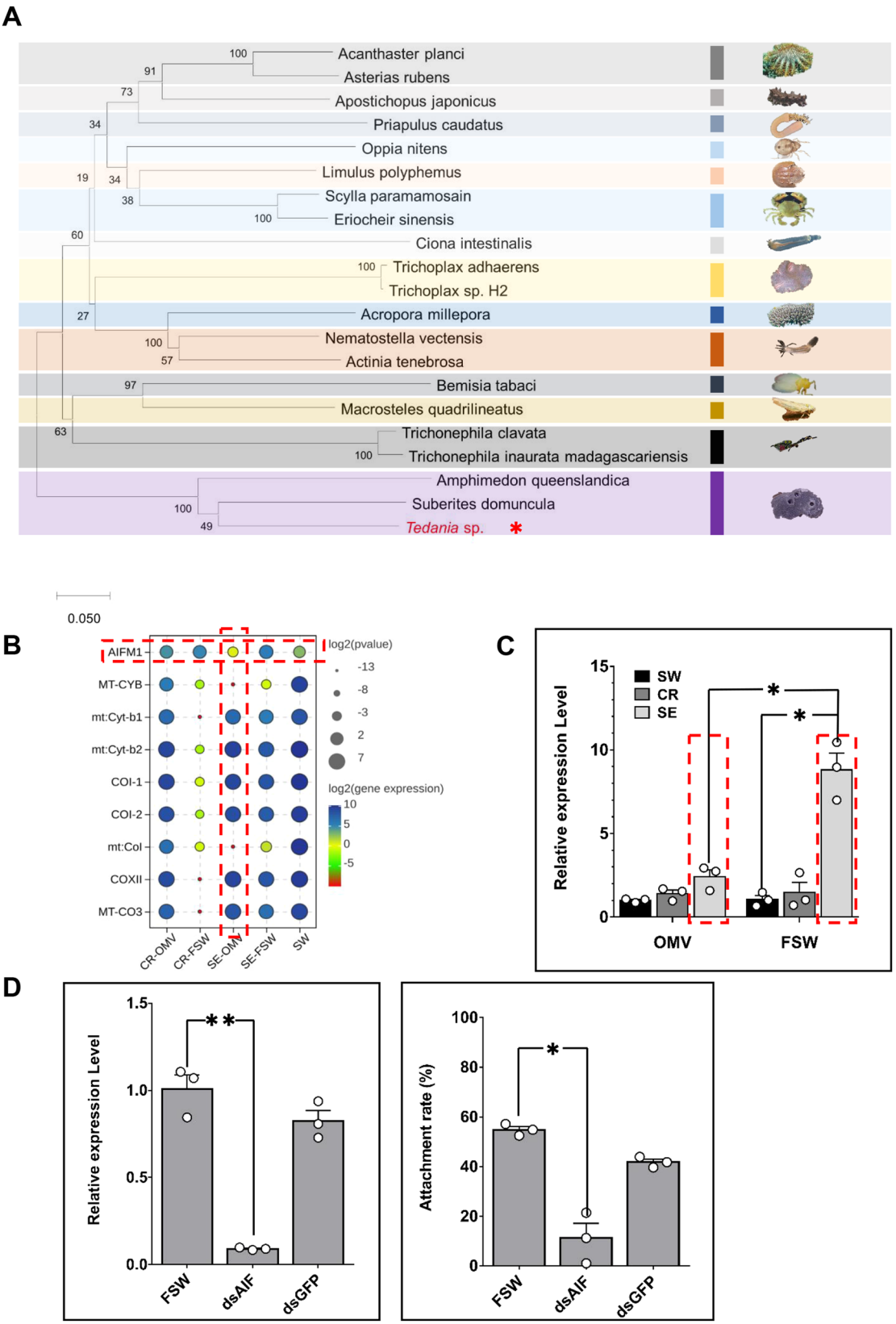

Fig. 3 | Functional verification of AIF regulation of larval settlement. **A** Phylogenetic analysis of *Te*-AIF against relatively similar AIF proteins from other animals. **B** Expression patterns of the DEGs related to oxidative phosphorylation and apoptosis in five samples of *Tedania* sp. **C** Analysis of the expression pattern of *Te-aif* in different groups using qRT-PCR. SW swimming larva, CR critical larva, SE settlement larva. For SW-FSW vs SE-FSW, *P*-value = 0.0196; For SE-OMV vs SE-FSW, *P*-value = 0.0378. **D** Relative expression level of the AIF mRNA after AIF siRNA interference. Larval attachment rate after RNAi of AIF. FSW: control group without any treatment. dsAIF: the group with the knockdown of high-concentration *Te-aif*. dsGFP: the group with the knockdown of high-concentration *gfp*. For the relative expression level of the AIF mRNA from the FSW group vs dsAIF group, *P*-value = 0.0086; For larval attachment rate in FSW group vs dsAIF group, *P*-value = 0.0119. Error bars represent one standard deviation from the mean of biological triplicate samples. *T*-test indicates statistical significance at $p \le 0.05$ (*), $p \le 0.01$ (**); $\alpha = 0.05$.

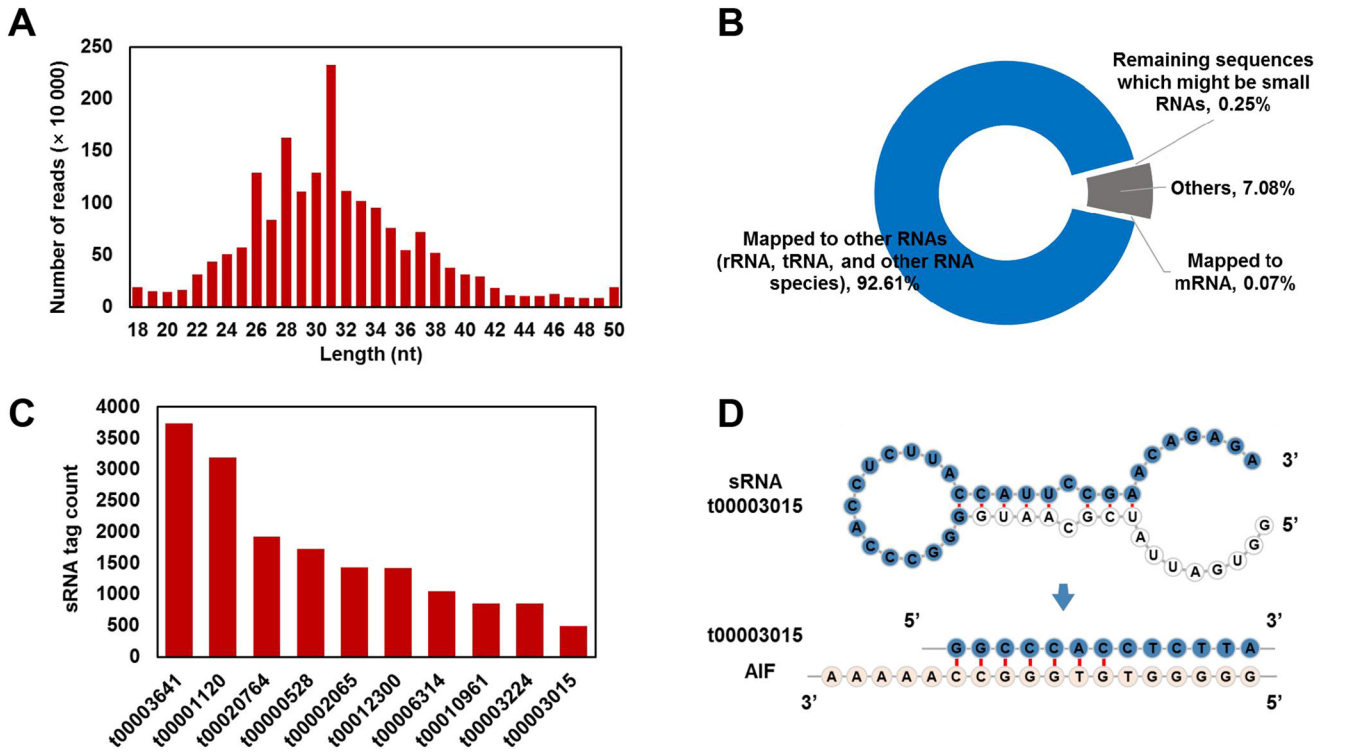

Fig. 4 | Identification of sRNAs and potential interactions between sRNAs and *aif* gene. **A** Length distribution of all sequences (mapped reads) in OMVs. **B** Annotation of clean data from OMVs. **C** Counts of high-abundance sRNAs. **D** Predicted secondary structures of t00003015 (highlights indicate the mature form of sRNAs) and the presumed target region in the *aif* gene.

Small RNAs in OMVs predicted to target the AIF mRNA

As a potential functional component affecting gene expression during host development, an analysis of small RNAs (sRNAs) in OMVs from *T. mesophilum* SP-7 was conducted. After filtering out the adaptor sequences and low-quality reads, 20,054,093 reads were selected as clean data and compared with the reference genome and RNA databases (Supplementary Table S5). The length distribution of all sRNAs (mapped reads) was in the 18–50 nt range, and most were between 25 and 38 nt (Fig. 4a). Moreover, rRNA, tRNA, and other RNAs comprised the vast majority of the clean data (92.61%), and approximately 0.06% of the total reads were from mRNA degradation (Fig. 4b). After excluding these sequences, the remaining sequences were considered putative sRNAs if they could form hairpins with flanking nucleotide sequences in the genome and if the secondary structure of the hairpins had minimum free energy ≤ 0 kcal/mol. Target genes of high-abundance sRNAs (count ≥ 100) (Fig. 4c) were predicted to identify potential interactions between OMVs-derived sRNAs and *Tedania* sp. mRNAs. Interestingly, the *aif* gene is a potential target of the sRNA t00003015, indicating that OMVs-derived sRNAs can be transported to host cells and inhibit apoptosis (Fig. 4d). These data preliminarily revealed that AIF-sRNAs were derived from bacterial OMVs and possibly downregulated *aif* gene expression after entering sponge cells.

Observation of sponge larvae at the SE developmental stage using TEM

We employed TEM to observe the sponge larvae in the SE-FSW and SE-OMV groups to further investigate the impact of bacterial OMVs on larval settlement (Fig. 5). The presence of apoptotic bodies, which only contained organelles (mitochondria and endoplasmic reticulum) and ranged in size from 1-5000 nm[31], was detected in both the SE-FSW and SE-OMV samples, suggesting that apoptosis occurred during the larval settlement stage. Due to technical limitations, the quantity of apoptotic bodies was difficult to assess accurately. Interestingly, bacterial internalization through endocytosis was also observed using TEM, suggesting that bacteria or OMVs likely enter sponge cells (more results can be found in Supplementary Fig. S6).

Discussion

Among the simplest multicellular animals abundant in seas and at various depths, one of the most notable characteristics of sponge holobionts is their interaction with the microbial world[32]. Bacterial symbionts were reported to play a crucial role in larval settlement through the formation of biofilms, and the release of semiochemicals[15]. Bacterial OMVs are ubiquitously produced and encapsulate soluble periplasmic content to transferring functional materials between cells[33]. According to a relevant report, the vesicle abundances in the coastal surface water was ~6×10^6 ml^{-1}, similar to the concentrations of bacteria at these sites[34]. In this study, we investigated the dose-dependent impact of bacterial OMVs on the development of marine sponges, in which the AIF-mediated apoptosis signaling pathway was modulated by possible bacterial sRNAs to influence larval settlement. Apoptosis-inducing factor (AIF) was identified nearly three decades ago, and an AIF-mediated caspase-independent cell death pathway has also been defined[35]. Much of the knowledge about AIF has come from AIF orthologs in model organisms, such as *Saccharomyces cerevisiae*, *Caenorhabditis elegans*, *Drosophila melanogaster* and mice[36–39], but no studies on apoptosis-inducing factor (AIF) in sponges have been reported. Here, we explored the role of AIF in the apoptosis signaling pathway, with a particular emphasis on sponge larval settlement.

Apoptosis occurs sequentially to ensure a homeostatic balance between cell formation and cell death. This process plays an essential role in regulating growth and development[40], such as the early development of chicken embryos[41] and the metamorphosis of *Clytia hemisphaerica* larvae[42]. The transition of larvae from swimming to settling is indispensable for sponges, who, as adults, are benthic. During the life cycle, most of the larvae die, and others start to settle into a new stage. AIF, which acts as a regulatory gene in oxidative phosphorylation and apoptosis, can maintain a balance between cell metabolism and cell death at the gene expression level[43]. The results of our qPCR and RNAi experiments also provided evidence that AIF influences apoptosis signaling pathways by regulating its own expression levels. During the process from swimming to settlement of larvae, *aif* expression continued to increase to eliminate some unhealthy larval cells, but when the larvae successfully settled,

aif expression was downregulated via OMVs. We speculated that maintaining a lower level of *aif* expression is conducive to sustained growth and development, in which cells maintained homeostasis via cell apoptosis mediated by AIF.

As reported in the literature, bacterial OMVs play a variety of functional roles, yet the ultimate function of OMVs is determined by their unique cargos, such as proteins, lipids and genetic material[44]. In this study, we found that many sRNAs derived from the bacterial strain *T. mesophilum* had access to host cells via OMVs. Bacterial OMVs contain differentially packaged sRNAs with the potential to target host mRNA function and/or stability[45,46]. Furthermore, an analysis of the sRNAome of OMVs revealed that the *aif* gene was a potential target of the sRNA t00003015. Compared to other cargos of OMVs, such as proteins and lipids[19], sRNAs appear to more directly regulate host gene expression and multiple signaling pathways. OMVs that act on hosts via bacterial sRNAs have been studied in recent

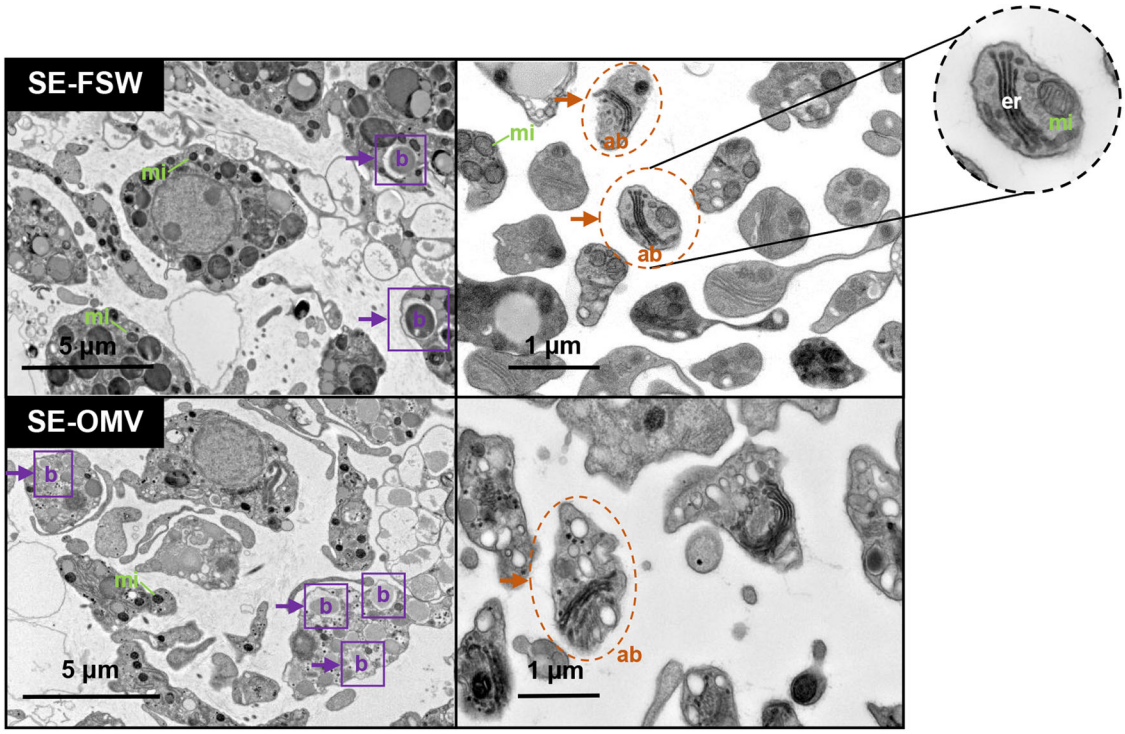

Fig. 5 | Transmission electron microscopy (TEM) observations of *Tedania* sp. larvae. TEM images of SE-FSW and SE-OMV samples of *Tedania* sp.; mi (green): mitochondria; er (white): endoplasmic reticulum; b (purple): bacteria were internalized by endocytosis; ab (orange): similar to apoptotic body; Scale bar: 5 μm (left) and 1 μm (right).

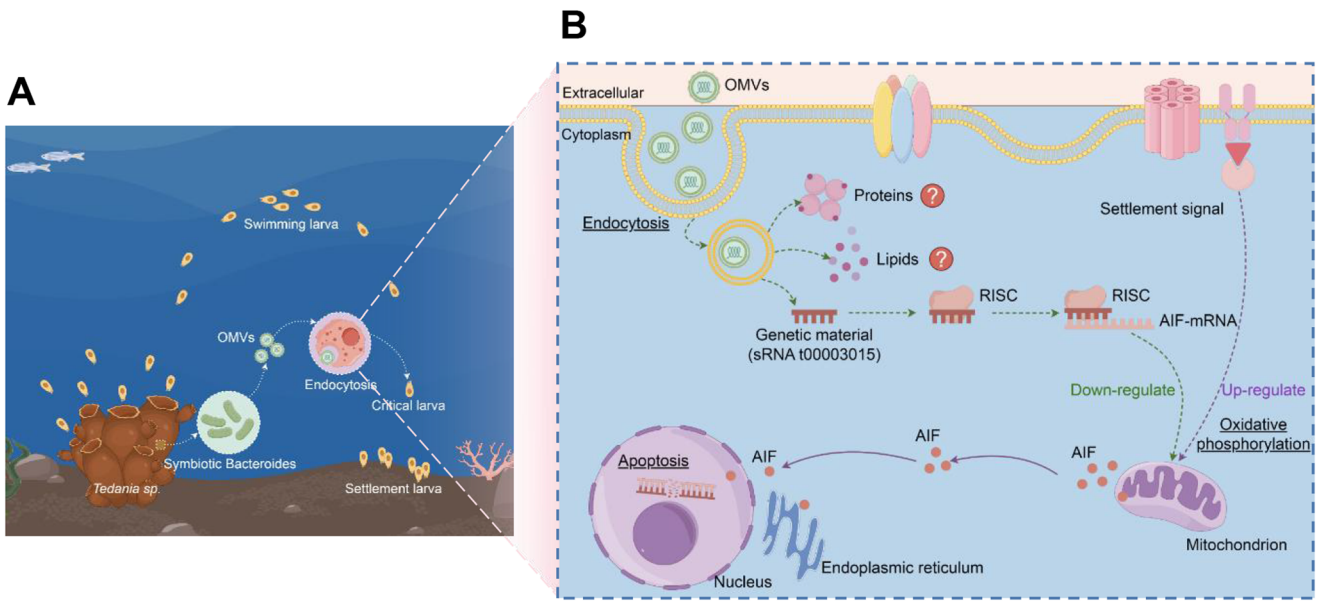

Fig. 6 | Schematic diagram of the mechanism by which OMVs induce larval settlement in *Tedania* sp. A The process of larval settlement in *Tedania* sp. **B** AIF-sRNAs (sRNA t00003015) derived from bacterial OMVs regulate apoptosis and promote larval settlement. OMVs outer membrane vesicles, AIF apoptosis-inducing factor, RISC RNA-induced silencing complex, AIF-mRNA AIF mRNA. This figure was drawn using Figdraw.

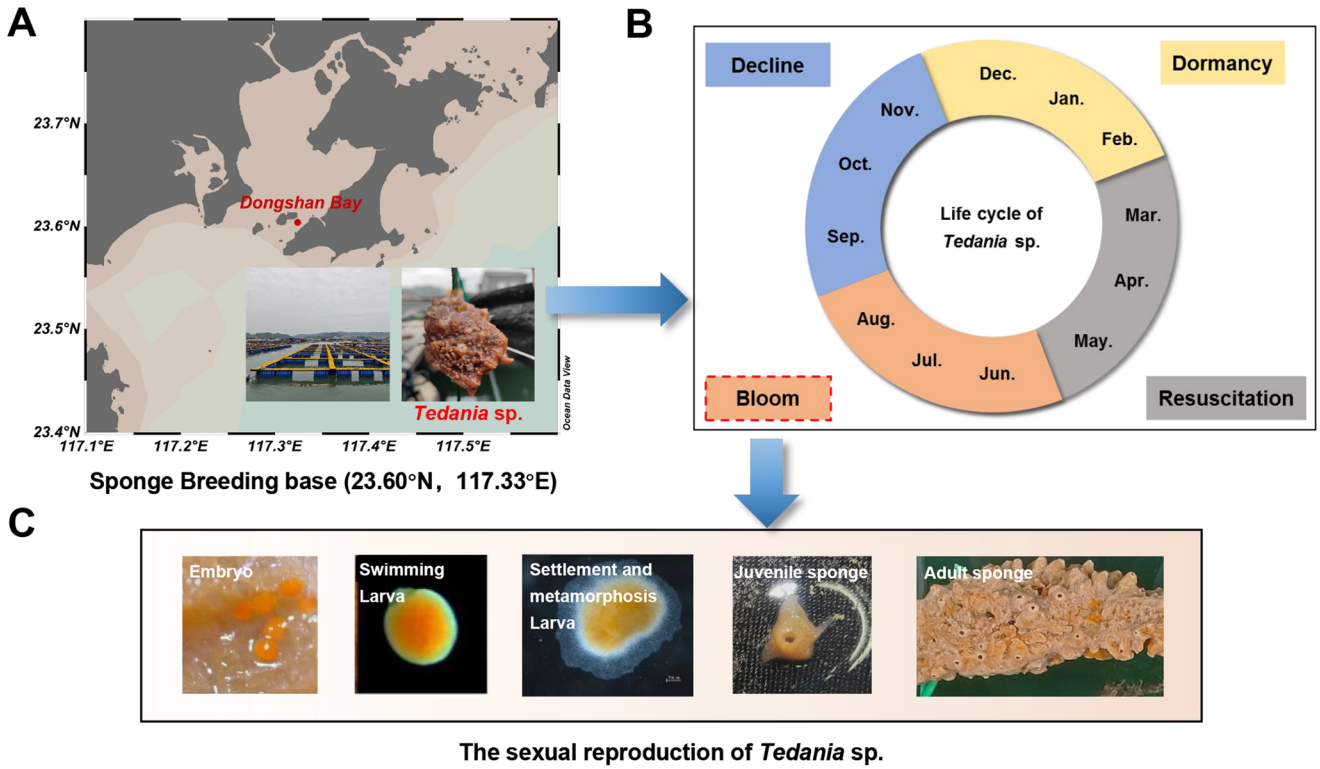

Fig. 7 | The life cycle of *Tedania* sp. A Sample collection site: Dongshan Bay (Fujian, China) on the west bank of the Taiwan Strait, indicated by a dot. **B** The life cycle of *Tedania* sp. **C** The developmental stages of the sexual reproduction of *Tedania* sp.

years, yet related research has focused on the immune response and pathology. *Pseudomonas aeruginosa* OMVs-packed sRNAs can regulate innate immune responses in mice[47]. The candidate sRNA (Xosr001) packaged in OMVs from the phytopathogen *Xanthomonas oryzae* functions to suppress stomatal immunity in rice[48]. Nevertheless, no studies are available on the biological development of OMVs-packed sRNAs. Here, the possible mutualistic mechanism, in which bacterial sRNAs are transported to the host via OMVs, provides a widely applicable means of exchanging substances for bacteria and further influences host growth and development[49].

Based on these results, we propose a hypothesis for the mechanism by which OMVs induce the larval settlement of *Tedania* sp. (Fig. 6). From the swimming to settlement stages, especially critical settlement, the abundance of specific microbial communities, such as Bacteroides, significantly increases to assist in host development[50]. Concurrently, these Bacteroides species release abundant OMVs containing sRNAs, e.g., AIF-sRNAs, and then OMVs are internalized by host cells, possibly through endocytosis. Finally, the AIF-sRNAs derived from Bacteroides regulate the apoptosis signaling pathway of the host, leading to successful larval settlement. Although evidence supporting this potential mechanism is available, host–microbe interactions are complicated processes, and much remains unknown, including the entry of bacterial OMVs into cells, the precise dose-dependent regulation of OMVs, and the specific cell types targeted by OMVs. The emergence of bacterial OMVs as distinct cellular entities could help bacteria adapt to diverse niches and, more importantly, play a crucial role in host-bacteria interactions[51].

For marine sponges, symbiosis has been researched for more than a century, but the mechanism by which symbionts are involved in larval settlement remains elusive[52]. Here, we propose that bacterial OMVs influence *Tedania* sp. larval settlement by modulating the AIF-mediated apoptosis signaling pathway. Furthermore, we determined through small RNA sequencing that the specific cargo transported by OMVs was AIF-sRNAs, which changed *aif* expression levels in the host. The effect of the *aif* gene, with a particular emphasis on larval settlement, was verified through qRT-PCR and RNAi experiments. In addition, the observation of samples using TEM implied that bacteria could be internalized through endocytosis. The settlement of marine invertebrate larvae is dynamic and intricate, and future research should focus on the molecular mechanism of the AIF-mediated apoptotic signaling pathway involved in larval settlement.

Materials and methods

Sampling

Tedania sp. was cultured at a designated site located in Dongshan Bay, Fujian Province, China (117.33E 23.60 N). The experimental field encompassed multiple net cages with plastic ropes perpendicular to the surface of the sea up to approximately 3 meters, which facilitated the settlement of larvae and the growth of adult sponges (Fig. 7a). *Tedania* sp. experiences typical life cycles with seasonal changes, including resuscitation (March to May), bloom (June to August), decline (September to November), and dormancy (December to February) (Fig. 7b). The sexual reproduction of *Tedania* sp. involves a series of programmed developmental stages: embryo, swimming larva, settlement and metamorphosis larva, juvenile, and adult (Fig. 7c). Larvae samples were collected from the swimming to settlement stages during the breeding period (bloom), such as from the SW, which represents the swimming larvae after release to water; from the CR, which refers to the competent larvae critical to settlement; and from the SE, which refers to the larvae settling on the surface, to study the effect of bacterial OMVs on larval settlement.

Larval attachment assay

The free-swimming larvae were trapped by a tuck net with a mesh screen (150 μm) and then cultured with naturally filtered seawater (filtered with 0.45 and 0.22 μm filter membranes). *Tenacibaculum mesophilum*, which belongs to Bacteroidetes and produces OMVs, was isolated from the sponge *Tedania* sp. and cultivated aerobically in marine 2216E broth (Solarbio, Beijing, China.) at 28 °C [30]. OMVs were isolated from 500 ml of bacterial culture (OD_{600} = ~1.0) in accordance with a modified procedure[53]. After all bacterial cells were removed via centrifugation at 5000 rpm for 30 min, the

Table.1 | Primers for qRT–PCR and RNAi

Primer name	Primer sequence	Product length (bp)
AIF-RT-F	CCGAAGCTGGGCCGCAGGAGA	285
AIF-RT-R	GCCTAGAATGCACCCTGCGTC	
SDHA-RT-F	TTTGCTGCAGAAGCCAGGAAG	230
SDHA-RT-R	CACACTGGGGCACACATCTTC	
AIF-RNAi-F	GATCACTAATACGACTCACTATAGGGGCTAGCAGAGGGAAGTCTCG	545
AIF-RNAi-R	CCATCAATGATCCCGGTGGC	
GFP-RNAi-F	GATCACTAATACGACTCACTATAGGGGAAGGTGATGCAACATACGGA	520
GFP-RNAi-R	GGGCAGATTGTGTGGACAG	

OMVs were separated from other extracellular products by ultracentrifugation at 100,000 × *g* for 1 h at 4 °C[13]. The amount of OMVs corresponding to the protein content was determined using a modified Bradford protein assay kit (Sangon Biotech, Shanghai, China.)[54]. Then, the bacterial OMVs were diluted with PBS (Solarbio, Beijing, China.) to various concentrations (0.08, 0.8, and 8 μg/mL). According to the developmental time of the larvae from swimming to settlement, the process was artificially divided into three stages: swimming larvae (SW, 0 h), critical larvae (CR, ~6 h after release to water), and settled larvae (SE, ~9 h after release to water). The experiment involved two groups, CR-FSW and SE-FSW, which represented the control groups with larvae in filtered seawater, and CR-OMV and SE-OMV, which represented the larvae in filtered seawater treated with OMVs. Different concentrations of OMVs were added to a six-well plate at the SW (0 h) stage, while the control group was not treated with OMVs. Each parallel plate had 30 larvae, and six parallel plates were set for each trial group. After 9 h, the number of settled larvae was counted every hour to evaluate the larval settlement rate.

RNA extraction, library construction and sequencing

For RNA sequencing (RNAseq), five samples (SW, CR-FSW, CR-OMV, SE-FSW, and SE-OMV) of *Tedania* sp. larvae with three biological replicates per sample were collected ($n = 15$ in total). According to the experimental method used for the larval attachment assay, a total of 180 larvae were collected per sample in theory, while ultimately, ~150 larvae were collected per sample for total RNA extraction due to the phenomenon of larval death during settlement. After being transported to the laboratory, the samples were rapidly frozen in liquid nitrogen and stored in a −80 °C freezer until the extraction process was completed. Moreover, total RNA was extracted using the Qiagen miRNeasy Mini Handbook (Germany)[55]. RNA quality was assessed on an Agilent 2100 Bioanalyzer (Agilent Technologies, Palo Alto, CA, USA) and checked using RNase-free agarose gel electrophoresis. After total RNA was extracted, eukaryotic mRNA was enriched with oligo(dT) beads, while prokaryotic mRNA was enriched by removing rRNA with a Ribo-Zero™ Magnetic Kit (Epicenter, Madison, WI, USA). Then, the enriched mRNA was fragmented into short fragments using a fragmentation buffer and reverse transcribed into cDNA with random primers. Second-strand cDNA was synthesized using DNA polymerase I, RNase H, dNTPs and buffer. Then, the cDNA fragments were purified with a QiaQuick PCR extraction kit (Qiagen, Venlo, The Netherlands), end-repaired, subjected to poly(A) addition, and ligated to Illumina sequencing adapters. The ligation products were size selected by agarose gel electrophoresis, PCR amplified, and sequenced using an Illumina HiSeqTM 4000 by Gene Denovo Biotechnology Co. (Guangzhou, China).

Comparative transcriptome analysis

The reads were further filtered with fastp[56] (version 0.18.0) to obtain high-quality reads. The high-quality clean reads were mapped to the full-length transcriptome of *Tedania* sp. using RSEM[57] (http://deweylab.github.io/RSEM/), and the gene abundances were calculated and normalized to RPKM. For each transcription region, the RPKM value was calculated to quantify its expression abundance and variations using RSEM software. Principal component analysis was performed with R package models (http://www.r-project.org/). Differentially expressed genes (DEGs) between the five samples were identified using DESeq2[58] software and edgeR[59]. The significant DEGs were compared between any two samples and screened using an FDR ≤ 0.05 and an absolute fold change ≥ 2. Afterward, DEGs were subjected to GO functional and KEGG pathway enrichment analyses, which were conducted using the OmicShare online tool with default parameters (https://www.omicshare.com/). Significant enrichment was defined as a *P* value < 0.05[60,61]. The protein–protein interaction network was identified using STRING v10, which recognized genes as nodes and interactions as lines in a network. Using Cytoscape (v3.7.1) software[62], the network file was visualized to display the biological interactions between the core and hub genes.

Sequence BLAST and phylogenetic analysis of potential apoptosis-inducing factors

Through the transcriptome analysis, a putative apoptosis-inducing factor (*Te-aif*) with a 1044 bp fragment from *Tedania* sp. larvae was selected to further investigate its relationship to larval settlement in more detail. The similarity between the target protein molecule and other AIF molecules was analyzed using the Web-based Basic Local Alignment Search Tool (BLAST) (http://blast.ncbi.nlm.nih.gov/Blast.cgi). Translation of the amino acid sequences and prediction of the deduced protein were performed with ExPASy (http://www.ExPASy.org). Alignments with homogenous sequences from other species were performed using MEGA 7.0. The phylogenetic analysis was performed using neighbor-joining (NJ) methods in MEGA 7.0 based on the amino acid sequences. The reliability was evaluated by selecting 1000 bootstraps for the NJ tree[63].

Data validation using quantitative real-time PCR (qRT–PCR)

The total RNA used for qRT-PCR was the same as that used for the RNA sequencing experiment and was obtained from the same batch of samples (SW, CR-FSW, CR-OMV, SE-FSW, and SE-OMV). Subsequently, RNA (~5 μg) from each sample reverse transcribed to the first strand of cDNA, which served as a template for PCR. The cDNA templates were diluted 10-fold in nuclease-free water and used as templates for the quantitative real-time PCR (qRT-PCR) analysis. The expression pattern of the *Te-aif* gene in various samples was studied using qRT-PCR according to the protocol of SYBR Premix Ex Taq (Takara, Japan). A pair of primers for *Te-aif* named AIF-RT-F and AIF-RT-R was designed and utilized for qRT-PCR (Table 1), and succinodehydrogenase (SDHA) was used as the internal reference[64]. qRT-PCR amplification was performed on a QuantStudio 6 Flex Real-Time PCR System (Bio-Rad, USA) in a volume of 12 μl containing 6 μl of 2 × TB Green Premix Ex Taq, 2 μl of 1:10 diluted cDNA, 1 μl (1 μM) of each primer, 0.3 μl of ROX Reference Dye II and 1.7 μl of ddH_2O. The qRT-PCR cycling conditions were as follows: 95 °C for 30 s and then 45 cycles of 95 °C for 5 s, 53 °C for 30 s and 72 °C for 20 s. Three parallel experiments were performed to increase the integrity. The comparative Ct method ($2^{-\Delta\Delta CT}$ method) was used to calculate the relative gene expression levels in the samples, which were normalized to the SDHA mRNA level. Differences in relative expression between consecutive stages were calculated, and a *t* test was performed using GraphPad Prism 7

(GraphPad Software, San Diego, CA, USA). Differences were considered statistically significant at a P value < 0.05.

RNA interference (RNAi) of the apoptosis-inducing factor (AIF) gene

Te-aif double strand RNA (dsRNA) was synthesized according to a previously reported method[65]; the specific primer sequences AIF-RNAi and GFP-RNAi (Table 1) were linked to the T7 promoter using a commercial transcription T7 kit (TaKaRa, Japan). The dsRNA synthesis system (with a 20 μl total volume) was devised according to the following methods: 1 μg of DNA template, 2 μl of 10 × transcription buffer, 2 μl each of A/U/C/GTP (50 mM), 0.5 μl of RNase inhibitor, and 2 μl of T7 RNA polymerase, which were mixed with RNase-free water to a total volume of 20 μl. After incubation at 42 °C for 2 h, the solution was added to a final volume of 3 μl with 2 μl of RNase-free DNase and 1 μl of RNase I. In addition, the mixed solution was incubated again at 37 °C for 1 h to remove the DNA templates and cut the dsRNA into siRNA. Subsequently, the dsRNA was extracted with phenol/chloroform, precipitated with ethanol, and then resuspended in 40 μl of RNase-free water. According to the instructions of the kit, siRNAs were synthesized in vitro, and *Te-aif* was knocked down using the AIF siRNA.

The sponge larvae were categorized into three distinct groups: the FSW group, the GFP dsRNA (dsGFP)-soaked group and the AIF dsRNA (dsAIF)-soaked group. Each group included 200 larvae and was provided with 16 mL of filtered seawater. In addition, the dsRNA injection group received an additional 100 μg/ml of siRNA[66], while no treatment was administered to the FSW group. After the knockdown of the *Te-aif* gene in vivo followed by siRNA challenge, larvae were extracted at 9 h (settlement) for RNA extraction. Along with counting the number of larvae attached, the first strand of cDNA, which was used as a template for PCR, was reverse transcribed using RNA from larvae. The mRNA expression levels of *Te-aif* were analyzed using the specific primers AIF-RT and SDHA-RT (Table 1). All measurements were repeated in triplicate. The relative expression ratio of the target genes to the reference gene was calculated using the $2^{-\Delta\Delta CT}$ method. SPSS software was used to analyze the obtained data, and all the data are presented as relative mRNA expression.

Transmission electron microscopy (TEM) observations of *Tedania* sp. larvae

Larval samples for TEM were fixed with 2.5% glutaraldehyde for 12 h in 0.22-μm-filtered seawater (FSW), postfixed with 1% osmium tetroxide for 2 h, dehydrated with 70%, 90%, and 100% ethanol, and the ethanol was replaced with ethanol: acetone (3:1, 1:1, and 1:3) in sequence for 15 min each time. The samples were subsequently embedded in fresh Spurr's resin (SPI-Chem Low Viscosity "Spurr" Kits)[67]. When sections were taken through the spicules during sectioning, the sliced surface of the resin block was occasionally damaged. Because of this damage, the larval samples were subjected to a modified procedure in which they were soaked in 5% hydrofluoric acid for 15 min after fixation with 2.5% glutaraldehyde[68]. This treatment lessened the spicule-induced breakage of the sections, and the experiment then proceeded as usual. Finally, sections with a thickness of 70 nm were observed using a TEM (HITACHI HT7800, Japan).

Small RNA sequencing of bacterial OMVs

Total RNA was extracted from *T. mesophilum* SP-7 OMVs and purified using a microRNA isolation kit (Qiagen)[45]. RNA molecules in the size range of 18-50 nt were enriched by polyacrylamide gel electrophoresis. The 3' and 5' adapters were added, and the ligation products were reverse transcribed by PCR amplification. Then, the 140–160 bp PCR-amplified products were enriched to generate a cDNA library and sequenced using the Illumina NovaSeq 6000 platform by Gene Denovo Biotechnology Co. (Guangzhou, China). Low-quality reads and adapter sequences were excluded from the raw reads to obtain clean tags. The GenBank database, Rfam database, and *T. mesophilum* genome (http://www.ncbi.nlm.nih.gov/nuccore/NZ_LDOD01000001.1) were used to identify and remove other RNA sequences (rRNA, tRNA, and other fragments) from mRNA degradation products. The secondary structure and the minimum free energy of the remaining sRNAs were predicted using RNAfold WebSever (http://rna.tbi.univie.ac.at/cgi-bin/RNAWebSuite/RNAfold.cgi). The candidate target genes corresponding to the mRNA expression profiles were predicted using Miranda (version 3.3a; http://www.mirbase.org) and TargetScan (version 7.0; https://www.targetscan.org/vert_72/) software with the default parameters, and the intersections of the results were chosen as the sRNA target genes.

Statistical analysis and reproducibility

All statistics are described throughout the methods. Briefly, for all RNA-seq data we utilized a cutoff of FDR (or adjusted p-value) < 0.05. For qRT-PCR and RNAi results analysis as indicated in the methods we used T-test indicates statistical significance at $p \leq$ at p indicate ≤ 0.01 (**); α = 0.05. The error bars in the figures represent the standard deviation.

Reporting summary

Further information on research design is available in the Nature Portfolio Reporting Summary linked to this article.

Data availability

All data supporting the findings of this study are available within the paper and its Supplementary Information. The raw RNA–Seq data used in this study are available in the NCBI Sequence Read Archive (SRA) under BioProject accession number PRJNA1042850 and are available at the following URL (https://www.ncbi.nlm.nih.gov/bioproject/PRJNA1042850/). The original data in the data figures refer to Supplementary Data 1–10. More specifically, for source data underlying the larval attachment assay in Fig. 1A, please see supplementary data sheet 1. For source data underlying the RNAseq processed data in Figs. 1–3, please see supplementary data sheet 2–9. For source data underlying the qPCR and RNAi in Fig. 3, please see supplementary data sheet 10.

Received: 11 December 2023; Accepted: 23 July 2024;
Published online: 06 August 2024

References

1. Mark, E. H. Marine chemical ecology: chemical signals and cues structure marine populations, communities, and ecosystems. *Ann. Rev. Mar. Sci.* **1**, 193–212 (2009).
2. Gaines, S. & Roughgarden, J. Larval settlement rate: a leading determinant of structure in an ecological community of the marine intertidal zone. *Proc. Natl Acad. Sci. USA* **82**, 3707–3711 (1985).
3. Freckelton, M. L. et al. Bacterial lipopolysaccharide induces settlement and metamorphosis in a marine larva. *Proc. Natl Acad. Sci. USA* **119**, e2200795119 (2022). 3.
4. Ribes, M., Dziallas, C., Coma, R. & Riemann, L. Microbial diversity and putative diazotrophy in high- and low-microbial-abundance Mediterranean sponges. *Appl Environ. Microbiol.* **81**, 5683–5693 (2015).
5. Marchi, L. D. et al. A multi-bioassay integrated approach to assess antifouling potential of extracts from the Mediterranean sponge *Ircinia oros*. *Environ. Sci. Pollut. Res. Int.* **29**, 1521–1531 (2022).
6. Van Soest, R. W. et al. Global diversity of sponges (Porifera). *PLoS One* **7**, e35105 (2012).
7. Whalan, S. The role of photobehaviour in sponge larval dispersal and settlement. *PLoS One* **18**, e0287989 (2023). 10.
8. Hadfield, M. G. Developmental symbiosis: a sponge larva needs symbiotic bacteria to succeed on the benthos. *Curr. Biol.* **31**, R88–R90 (2021). 25.
9. Pankey, M. S. et al. Cophylogeny and convergence shape holobiont evolution in sponge-microbe symbioses. *Nat. Ecol. Evol.* **6**, 750–762 (2022).
10. Nadjejda, E. V. et al. Reduced seawater pH alters marine biofilms with impacts for marine polychaete larval settlement. *Mar. Environ. Res.* **167**, 105291 (2021).
11. Dobretsov, S. & Rittschof, D. Love at first taste: induction of larval settlement by marine microbes. *Int. J. Mol. Sci.* **21**, 731 (2020).

12. Song, H., Hewitt, O. H. & Degnan, S. M. Arginine biosynthesis by a bacterial symbiont enables nitric oxide production and facilitates larval settlement in the marine-sponge host. *Curr. Biol.* **31**, 433–437.e3 (2021).
13. Beibei, Z. et al. Multiomics integration for the function of bacterial outer membrane vesicles in the larval settlement of marine sponges. *Front Microbiol* **15**, 1268813 (2024).
14. Freckelton, M. L., Nedved, B. T. & Hadfield, M. G. Induction of invertebrate larval settlement; different bacteria, different mechanisms? *Sci. Rep.* **7**, 42557 (2017).
15. Whalan, S. & Webster, N. S. Sponge larval settlement cues: the role of microbial biofilms in a warming ocean. *Sci. Rep.* **4**, 4072 (2014).
16. Raposo, G. & Stahl, P. D. Extracellular vesicles: a new communication paradigm? *Nat. Rev. Mol. Cell Biol.* **20**, 509–510 (2019).
17. Lécrivain, A. L. & Beckmann, B. M. Bacterial RNA in extracellular vesicles: a new regulator of host-pathogen interactions? *Biochim. Biophys. Acta Gene Regul. Mech.* **1863**, 194519 (2020).
18. Keren, R. et al. Sponge-associated bacteria mineralize arsenic and barium on intracellular vesicles. *Nat. Commun.* **8**, 14393 (2017).
19. Guanju, W. et al. Outer membrane vesicles induce the mussel plantigrade settlement via regulation of c-di-GMP. *Biofouling* **39**, 359–370 (2023).
20. Aschtgen, M. S. et al. Rotation of vibrio fischeri flagella produces outer membrane vesicles that induce host development. *J. Bacteriol.* **198**, 2156–2165 (2016).
21. Woznica, A. et al. Bacterial lipids activate, synergize, and inhibit a developmental switch in choanoflagellates. *Proc. Natl Acad. Sci. USA* **113**, 7894–7899 (2016).
22. Mariana, G. S., Evan, J. P., Mario, F. F. & M Florencia, H. Bacterial outer membrane vesicles: from discovery to applications. *Annu. Rev. Microbiol.* **8**, 609–630 (2021).
23. Schatz, D. & Vardi, A. Extracellular vesicles-new players in cell-cell communication in aquatic environments. *Curr. Opin. Microbiol.* **43**, 148–154 (2018).
24. Pankaj, K., Jordan, A., Suresh, B. M. & Anindya, D. Meta-analysis of tRNA derived RNA fragments reveals that they are evolutionarily conserved and associate with AGO proteins to recognize specific RNA targets. *BMC Biol.* **1**, 78 (2014).
25. Roy, L. M. et al. tRNA-derived microRNA modulates proliferation and the DNA damage response and is down-regulated in B cell lymphoma. *Proc. Natl Acad. Sci. USA* **110**, 1404–1409 (2013).
26. Idrissa, D. et al. A tRNA-derived fragment present in *E. coli* OMVs regulates host cell gene expression and proliferation. *PLoS Pathog.* **18**, e1010827 (2022).
27. Jonathan, B. L. et al. Ambient pH alters the protein content of outer membrane vesicles, driving host development in a beneficial symbiosis. *J. Bacteriol.* **201**, e00319–e00319 (2019).
28. Tingting, W. et al. Proteus mirabilis vesicles induce mitochondrial apoptosis by regulating miR96-5p/Abca1 to inhibit osteoclastogenesis and bone loss. *Front Immunol.* **13**, 833040 (2022).
29. Obeng, E. Apoptosis (programmed cell death) and its signals—a review. *Braz. J. Biol.* **81**, 1133–1143 (2021).
30. Li, M. Y. et al. Bacteroidetes bacteria, important players in the marine sponge larval development process. *iScience* **24**, 102662 (2021).
31. Sweta, R., Aideen, E. R., Matthew, D. G. & Thomas, R. Mesenchymal stem cell-derived extracellular vesicles: toward cell-free therapeutic applications. *Mol. Ther.* **23**, 812–823 (2015).
32. Bright, M. & Bulgheresi, S. A complex journey: transmission of microbial symbionts. *Nat. Rev. Microbiol* **8**, 218–230 (2010).
33. Carmen, S. & Meta, J. K. Outer-membrane vesicles from Gram-negative bacteria: biogenesis and functions. *Nat. Rev. Microbiol.* **13**, 605–619 (2015).
34. Steven, J. B. et al. Bacterial vesicles in marine ecosystems. *Science* **343**, 183–186 (2014).
35. Céline, C., Francesco, C., Philippe, D., & Guido, K. Apoptosis-inducing factor (AIF): key to the conserved caspase-independent pathways of cell death? *J. Cell Sci.* 15;115(Pt 24):4727–4734 (2002).
36. Wissing, S. et al. An AIF orthologue regulates apoptosis in yeast. *J. Cell Biol.* **166**, 969–974 (2004).
37. Wang, X., Yang, C., Chai, J., Shi, Y. G. & Xue, D. Mechanisms of AIF-mediated apoptotic DNA degradation in *Caenorhabditis elegans*. *Science* **298**, 1587–1592 (2002).
38. Joza, N. et al. The molecular archaeology of a mitochondrial death effector: AIF in Drosophila. *Cell Death Differ.* **15**, 1009–1018 (2008).
39. Zhu, C. et al. Apoptosis-inducing factor is a major contributor to neuronal loss induced by neonatal cerebral hypoxia-ischemia. *Cell Death Differ.* **14**, 775–784 (2007).
40. Lockshin, R. A. & Zakeri, Z. Programmed cell death and apoptosis: origins of the theory. *Nat. Rev. Mol. Cell Biol.* **2**, 545–550 (2001).
41. Makino, K. et al. Apoptosis occurs during early development of the bursa of Fabricius in chicken embryos. *Biol. Pharm. Bull.* **37**, 1982–1985 (2014).
42. Krasovec, G., Pottin, K., Rosello, M., Quéinnec, É., & Chambon, J. P. Apoptosis and cell proliferation during metamorphosis of the planula larva of *Clytia hemisphaerica* (Hydrozoa, Cnidaria). Dev Dyn. 250:1739–1758 (2021).
43. Joza, N. et al. AIF: not just an apoptosis-inducing factor. *Ann. N. Y Acad. Sci.* **1171**, 2–11 (2009).
44. Niel, G. V., Angelo, G. D. & Raposo, G. Shedding light on the cell biology of extracellular vesicles. *Nat. Rev. Mol. Cell Biol.* **19**, 213–228 (2018).
45. Lily, A. C. et al. Bacterial outer membrane vesicles and immune modulation of the host. *Membranes* **13**, 752 (2023).
46. Katja, K. et al. A novel mechanism of host-pathogen interaction through sRNA in bacterial outer membrane vesicles. *PLoS Pathog.* **12**, e1005672 (2016).
47. Zhen, X. et al. Pseudomonas aeruginosa outer membrane vesicle-packed sRNAs can enter host cells and regulate innate immune responses. *Micro. Pathog.* **188**, 106562 (2024).
48. Yan, W. et al. Suppression of host plant defense by bacterial small RNAs packaged in outer membrane vesicles. *Plant Commun.* **12**, 100817 (2024).
49. Mengdan, H. et al. Insights into the regulatory role of bacterial sncRNA and its extracellular delivery via OMVs. *Appl. Microbiol. Biotechnol.* **108**, 29 (2024).
50. Wu, S., Ou, H., Liu, T., Wang, D., & Zhao, J. Structure and dynamics of microbiomes associated with the marine sponge Tedania sp. during its life cycle. *FEMS Microbiol. Ecol*. 1; 94 (2018).
51. Segaran, T. C., Azra, M. N., Lananan, F. & Wang, Y. Microbe, climate change and marine environment: linking trends and research hotspots. *Mar. Environ. Res.* **189**, 106015 (2023).
52. G, Seghal et al. Marine sponge microbial association: towards disclosing unique symbiotic interactions. *Mar. Environ. Res.* **140**, 169–179 (2018).
53. Kulp, A. & Kuehn, M. J. Biological functions and biogenesis of secreted bacterial outer membrane vesicles. *Annu. Rev. Microbiol.* **64**, 163–184 (2010).
54. Klimentová, J. & Stulík, J. Methods of isolation and purification of outer membrane vesicles from gram-negative bacteria. *Microbiol Res* **170**, 1–9 (2015).
55. Strehlow, B. W., Schuster, A. W., & Francis, R. Transcriptomic responses of sponge holobionts to in situ, seasonal anoxia and hypoxia. bioRxiv. https://doi.org/10.1101/2023.02.27.530229 (2023).
56. Chen, S. F., Zhou, Y. Q., Chen, Y. R. & Gu, J. fastp: an ultra-fast all-in-one FASTQ preprocessor. *Bioinformatics* **34**, i884–i890 (2018).
57. Li, B. & Dewey, C. N. RSEM: accurate transcript quantification from RNA-Seq data with or without a reference genome. *BMC Bioinforma.* **12**, 323 (2011).

58. Love, M. I., Huber, W. & Anders, S. Moderated estimation of fold change and dispersion for RNA-seq data with DESeq2. *Genome Biol.* **15**, 550 (2014).
59. Robinson, M. D., McCarthy, D. J. & Smyth, G. K. edgeR: a Bioconductor package for differential expression analysis of digital gene expression data. *Bioinformatics* **26**, 139–140 (2010).
60. Ashburner, M. et al. Gene ontology: tool for the unification of biology. *Nat. Genet.* **25**, 25–29 (2000). The Gene Ontology Consortium.
61. Liao, L. Q. et al. Transcriptomic analysis reveals the dynamic changes of transcription factors during early development of chicken embryo. *BMC Genom.* **23**, 825 (2022).
62. Shannon, P. et al. Cytoscape: a software environment for integrated models of biomolecular interaction networks. *Genome Res.* **13**, 2498–2504 (2003).
63. Wiens, M. et al. Induction of gene expression of the chaperones 14-3-3 and HSP70 by PCB 118(2,3'4,4',5-pentachlorobiphenyl) in the marine sponge Geodia cydonium: novel biomarkers for polychlorinated biphenyls. *Mar. Ecol. Prog. Ser.* **165**, 247–257 (1998).
64. Ren, B. et al. Enantioselective toxic effects of the novel chiral antifungal agrochemical penthiopyrad in the early life stage of zebrafish (Danio rerio). *Chem. Biol. Interact.* **369**, 110252 (2023).
65. Wang, K. et al. Molecular characterization and expression analysis of dopa decarboxylase involved in the antibacterial innate immunity of the freshwater crayfish, Procambarus clarkii. *Fish. Shellfish Immunol.* **91**, 19–28 (2019).
66. Rivera, A. S. et al. RNA interference in marine and freshwater sponges: actin knockdown in Tethya wilhelma and Ephydatia muelleri by ingested dsRNA expressing bacteria. *BMC Biotechnol.* **11**, 67 (2011).
67. Gloeckner, V. et al. The HMA-LMA dichotomy revisited: an electron microscopical survey of 56 sponge species. *Biol. Bull.* **227**, 78–88 (2014).
68. Ereskovsky, A. & Tokina, D. Ultrastructural research of spermiogenesis in two sponges, crellomima imparidens and hymedesmia irregularis (Demospongiae): new evidence of sperms with acrosome in sponges. *J. Morphol.* **283**, 333–345 (2022).

Acknowledgements

This research was supported by grants from the National Natural Science Foundation of China (grant number 41876183) and the Fundamental Research Funds for the Central Universities (grant number 20720200045). We would like to thank American Journal Experts for their linguistic assistance during the preparation of this manuscript.

Author contributions

Kai Wang conducted the experiments and wrote the paper; Chenzheng Jia analyzed the small RNA (sRNA) sequencing data; Beibei Zhang assisted in the collection of experimental samples; Jun Chen provided the experimental materials; and Jing Zhao directed the experimental design and writing of the article.

Competing interests

The authors declare no competing interests.

Additional information

Supplementary information The online version contains supplementary material available at https://doi.org/10.1038/s42003-024-06622-7.

Correspondence and requests for materials should be addressed to Kai Wang, Chenzheng Jia, Beibei Zhang, Jun Chen or Jing Zhao.

Peer review information *Communications Biology* thanks the anonymous reviewers for their contribution to the peer review of this work. Primary Handling Editor: Tobias Goris.